

## Valley Phase, Interface Roughness and Voltage Control, and Coherent Manipulation in Si Quantum Dots

Neil Zimmerman<sup>1\*</sup>, Peihao Huang<sup>1,2</sup>, Dimitrie Culcer<sup>†3</sup>

<sup>1</sup>*Quantum Measurement Division, National Institute of Standards and Technology, MD 20899, USA*

<sup>2</sup>*Joint Quantum Institute, University of Maryland and National Institute of Standards and Technology, MD 20742, USA and*

<sup>3</sup>*School of Physics, The University of New South Wales, Sydney 2052, Australia*

We point out that, with any roughness at the interface of an indirect-bandgap semiconducting dot, the phase of the valley-orbit coupling can take on a random value. We discuss how this uncontrolled phase, in double quantum dots, causes a large change in the exchange splitting. Furthermore, we show how the uncontrolled phase causes difficulties for the coherent manipulation of a singlet-triplet spin qubit, and for the entanglement of two single-spin qubits. We then show that, with lateral control of the position of a quantum dot using a gate voltage, the valley-orbit phase can be controlled over a wide range, so that variations in the exchange splitting can be controllably suppressed for individual devices. Finally, we suggest experiments to measure the valley phase and the concomitant gate voltage control.

Quantum coherent manipulation of electrons in Si has been a very active field of study recently[1][2]. The advantages of Si include low spin-orbit coupling and the ability to isotopically enrich <sup>28</sup>Si, both of which will tend to reduce the decoherence of spin qubits. In addition, the integration with CMOS classical circuitry holds the potential for monolithically integrating qubits with control circuits[2]. Very recent advances in demonstrating quantum coherence include driving single spins in SiGe quantum dots with micromagnets[3][4], single spins in Si/SiO<sub>2</sub> quantum dots including Stark-shifted addressability[5], and a two-qubit gate in Si/SiO<sub>2</sub> quantum dots[6].

One complication for quantum control in Si is engendered by the valley degree of freedom; there are six equivalent positions in the three-dimensional band structure[1]. Because there is no external control of the valley quantum number, complications include difficulty in well-defined initialization and enhanced spin decoherence at valley relaxation “hotspots”[7]. Experimental measurements of the magnitude of the valley splitting between the lowest two valley states include spin-valley “hotspots”[8] and valley splitting magnitude tunable with electric field[7][9].

Theoretical predictions of the valley-orbit coupling include predictions of magnitude in perfect SiGe[10][11][12][13] and SiO<sub>2</sub>[14][15], magnitude in disordered interfaces[16][17][18], effects of valley phase on magnitude[19][20][21], spin-valley interactions[22][23] and intervalley dynamics at interface steps[24].

In the vicinity of an interface, the lowest energy valleys are typically perpendicular to the interface, and are split

by the valley-orbit coupling, which is defined as

$$\Delta = \langle z | (\mathcal{V} + eFz) | \bar{z} \rangle, \quad (1)$$

where  $|z\rangle$ ,  $|\bar{z}\rangle$  are the bare valley states centered at  $k_z = \pm k_0 = \pm(0.85)2\pi/a_0$ ,  $\mathcal{V}$  is the interfacial potential energy,  $F$  is the applied electric field, and  $a_0$  is lattice constant; this leads to eigenstates which are symmetric superpositions of  $|z\rangle$  and  $|\bar{z}\rangle$  (see text above Eqn 7), split by  $|\Delta|$ . We note that, by virtue of the definition, the coupling is a complex quantity  $\Delta = |\Delta|e^{i\phi}$ . In contrast to the magnitude, there has been little consideration of the complex phase[19][20][21]  $\phi$ . Although the global phase  $\phi$  for a single quantum dot or donor has no physical consequence, as we will show in this paper the phase difference  $\Delta\phi$  between two quantum dots or donors has great significance, because matrix elements (such as exchange splitting) between the two dots depend on  $\Delta\phi$ .

As in studies of the magnitude of the valley splitting, the roughness of the interface is the crucial device feature; this is because the Bloch wavefunction is tied to the Si lattice, while the envelope of the electron wavefunction follows the rough interface. With  $d = a_0/4$  the thickness of a single terrace step,  $2k_0d \approx 2(0.85)(2\pi/a_0)(a_0/4) \approx 0.42(2\pi)$ . Thus, not only is the value of  $\phi$  large, it is also incommensurate with  $2\pi$ ; this basic fact is the origin of the large effects discussed in this paper.

The main point of this paper is the qubit gate operation frequencies can both i) change by orders of magnitude depending on small details of the interface roughness, and ii) can be controlled by orders of magnitude with gate voltage control. This occurs because, as we will show, the exchange splitting  $J \propto 1 + \cos \Delta\phi$ . Thus, the large value of  $\Delta\phi$  manifests itself as an unpredictable  $\sigma_z$  rotation frequency ( $J/h$ ) for both two electrons on two dots (2e2d) singlet-triplet qubits and two-qubit gate coupling frequency ( $J/h$ ) for 2e2d single spin qubits; these effects are present for both interfaces with steps (corresponding to Si/SiGe) and with random fluctuations

\*+1-301-975-5887; neilz@mailaps.org;  
ftp://ftp.nist.gov/pub/physics/neilz/papers.html  
†d.culcer@unsw.edu.au

(Si/SiO<sub>2</sub>).

In this paper, we will show (within the effective mass approximation) i) the derivations of  $\Delta\phi$  based on interface roughness and the dependence of  $J$  on  $\Delta\phi$ , ii) results of simulations of  $\Delta\phi$  for both step and random interfaces, and iii) the ability to control the coupling phase with applied gate voltage, by laterally shifting quantum dots.

We consider an electron in a quantum dot, localized in the  $z$ -direction by the combination of interface and accumulation gate voltage, and localized in the  $x$ -,  $y$ -directions by lateral gates. The potential is then

$$V_D(x, y, z) = \frac{\hbar^2}{2m^*a^2} \left[ \frac{(x - x_D)^2 + y^2}{a^2} \right] + \mathcal{V}(x, y, z) + eFz, \quad (2)$$

The QD has a Fock-Darwin radius  $a$ , with  $m^*$  the Si in-plane effective mass. The effective mass (EMA) single-electron wavefunctions for a multi-valley system are

$$L_z(x, y, z) = \phi_L(x, y) \psi(z) u_z(\mathbf{r}) e^{ik_0z}, \quad (3)$$

and similarly for position R and valley  $\bar{z}$  (L and R are the two lateral locations of the quantum dots); here,  $\psi(z)$  is the envelope function for the  $z$ -direction and  $u_z(\mathbf{r})$  has the periodicity of the lattice. Using  $D = \{L, R\}$ ,

$$\phi_D(x, y) = \frac{1}{a\sqrt{\pi}} e^{-\frac{(x-x_D)^2+y^2}{2a^2}}. \quad (4)$$

Finally, the interface potential is

$$\mathcal{V}(x, y, z) = U_0 \theta[\zeta(x, y) - z], \quad (5)$$

where  $\zeta(x, y)$  is the height of the rough interface. With this interface, we make the assumption that the center-of-charge of the wavefunction follows exactly:  $\psi(z) \rightarrow \psi(z - \zeta)$ . This assumption is justified when the variation of  $\zeta(x, y)$  with respect to  $x, y$  is not too large (see Supplement). Combining this with Equations 1, 3, 6, we obtain

$$\Delta_D \approx \Delta_0 \int_{-\infty}^{\infty} \int_{-\infty}^{\infty} dx dy |\phi_D(x, y)|^2 e^{-2ik_0\zeta(x, y)}, \quad (6)$$

where  $\Delta_0$  is the valley splitting in the absence of interface roughness. Finally we define  $\Delta_{L,R} = |\Delta_{L,R}| e^{-i\phi_{L,R}}$  and  $\Delta\phi = \phi_L - \phi_R$ . We note that the assumption of pure position states L and R is equivalent to assuming the Coulomb repulsion energy is large compared to the tunneling energy, which is generally experimentally valid. A simple consequence of Equation 6: If we consider a flat interface with one step of height  $d$  located between the two dots, because  $\zeta$  is defined with respect to the underlying Si lattice,  $\Delta\phi = 2k_0d$ , as discussed above.

We now turn to the dependence of exchange energy on valley phase: After mixing  $|z\rangle$  and  $|\bar{z}\rangle$  through the valley splitting, the single-particle states are  $|L_{\pm}\rangle = \frac{1}{\sqrt{2}}(|L_z\rangle \pm e^{i\phi_L}|L_{\bar{z}}\rangle)$ , and similarly for R. Thus, the tunneling matrix element between lowest-lying states  $t_{--} =$

$t_{++} = \langle L_-|T|R_- \rangle$  is

$$\begin{aligned} t_{--} &= \frac{1}{2}(\langle L_z| - e^{-i\phi_L}\langle L_{\bar{z}}|)T(|R_z\rangle - e^{i\phi_R}|R_{\bar{z}}\rangle) \\ &= \frac{1}{2}[\langle L_z|T|R_z\rangle + e^{-i\Delta\phi}\langle L_{\bar{z}}|T|R_{\bar{z}}\rangle] = \frac{t_0}{2}[1 + e^{-i\Delta\phi}], \end{aligned} \quad (7)$$

where  $T$  and  $t_0$  are the tunneling Hamiltonian, and the tunneling matrix element in the absence of valley effects, respectively. Similarly,  $t_{-+} = \frac{t_0}{2}[1 - e^{-i\Delta\phi}]$ . The exchange energy  $J = 4|t_{--}|^2/U$ , where  $U$  is the on-site repulsion energy, and thus

$$J = \frac{J_0}{2}(1 + \cos \Delta\phi), \quad (8)$$

where  $J_0 = 4|t_0|^2/U$  is the exchange energy in the absence of valley phase.

Figure 1 shows the results for simulated SiGe interfaces (horizontal sections separated by vertical steps) for both random (approximately equal numbers of upgoing and downgoing steps) and for vicinal (all steps are upgoing) interfaces. The interfaces were generated by assigning steps at random lateral positions so as to get a particular average lateral density, as indicated in the graphs. As shown, for any roughness,  $\Delta\phi$  is of large magnitude compared to  $2\pi$ , and has no systematic dependence on tilt or randomness; these facts both occur because, as discussed above,  $2k_0d$  is large for a single terrace step.

Similar to Figure 1, Figure 2 shows the calculation for  $\Delta\phi$  appropriate for a Si/SiO<sub>2</sub> interface without and with vicinal tilt. We generated this interface by i) first generating a random Fourier transform of variable width  $\Delta\lambda$ , ii) inverse Fourier transforming, and then iii) scaling to give a total vertical height of about 1.5 nm (equivalent to the height of 10 random steps in Figure 1a). In Figure 2a), zero width corresponds to a single correlation length of 20 nm (sinusoidal roughness), and the largest width  $\Delta\lambda = 100$  corresponds to a range of correlation lengths between two and 20 nm. Previous high resolution TEM and weak localization studies of the Si/SiO<sub>2</sub> interface have yielded a range of correlation lengths from a few nm[25] up to 100 nm[26][27]. We see that, as for the SiGe interface, vicinal and non-vicinal randomness with a variety of correlation lengths all lead to large values of  $\Delta\phi$ .

We now turn to the implications of these large complex valley phase differences for coherent manipulation: Figure 3 lower panel shows the results of Equation 8 for the exchange energy  $J$ , and also for the inter-valley tunneling probability  $t_{-+}$ , for a Si/SiO<sub>2</sub> interface with a range of correlation lengths. We see that, as expected, the large values of  $\Delta\phi$  correspond to large deviations in  $J$  from its nominal value. For interfaces with random and stepped roughness of typical density, this indicates that there will be a large uncontrolled deviation in the exchange energy, and thus a large uncontrolled deviation in the single-gate rotations of singlet/triplet qubits, and in the two-gate interactions of single-spin qubits. The similar uncontrolled variation in  $t_{-+}$  may correspond to an analogous uncontrolled initialization of a particular valley state.

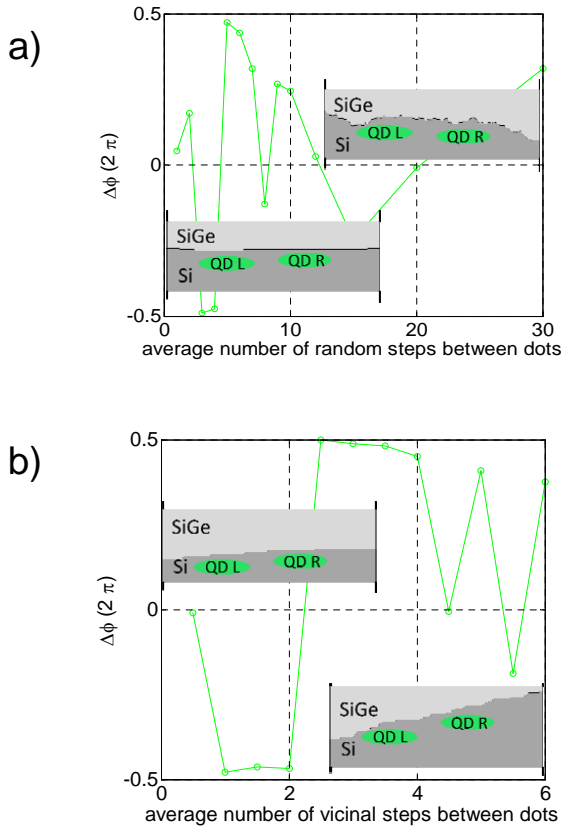


FIG. 1: Calculation of  $\Delta\phi$  for Si/SiGe interfaces (horizontal sections separated by vertical steps), for two types of simulated interfaces: a) Interface is on average horizontal, and contains upgoing and downgoing steps randomly distributed with a lateral density as indicated; b) Interface is tilted (vicinal), with only upgoing steps randomly distributed as indicated. Insets are sketches of representative interfaces at the two ends of the ranges of lateral densities. Note that  $\Delta\phi$  is large for all rough interfaces, because  $2k_0 a_0/4$  is large.

We now turn to reducing or eliminating this uncontrolled deviation with an experimental control. Since the valley phase in Equation 6 arises from the vertical height of the interface, at first glance one might think that moving the dot vertically into the Si substrate might have a strong effect on  $\Delta\phi$ ; although a vertical electric field has strong effect on the magnitude of the coupling<sup>[9]–[21]</sup>, it has a negligible effect on  $\Delta\phi$ <sup>[14][21]</sup>. However, due to the strong dependence of the valley phase on the exact local realization of the interface roughness, using a gate voltage to shift the dot laterally can have a large effect.

Overall, Figure 3 shows this possibility: the upper panel shows the effect on  $\Delta\phi$  of moving both dots laterally with a constant separation, for both a sinusoidal interface ( $\Delta\lambda = 0$ ) and random interface ( $\Delta\lambda = 10$ ). Clearly, the phase difference  $\Delta\phi$  and the concomitant energies are strong functions of the lateral position; this is simply because moving a dot changes the local interface

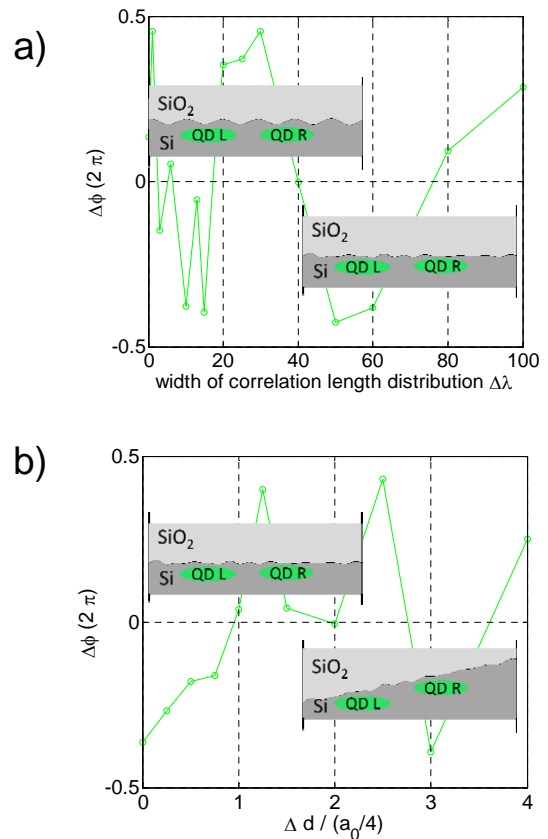


FIG. 2: Calculation of  $\Delta\phi$  for Si/SiO<sub>2</sub> interfaces: a) Interface is on average horizontal, and is generated by inverse Fourier transform of a randomly generated function of variable width. Larger width yields a more random interface, as indicated by the inset sketches. b) Similar to a), using a single random interface and a variable amount of vicinal tilt;  $\Delta d$  is the vicinal height difference between the two dots, so that  $\Delta d/(a_0/4)$  is the height difference in units of equivalent terrace steps (compare to Figure 1). Note that the interface is not flat at the left end of both graphs, so that  $\Delta\phi$  is nonzero there.

height, and thus the phase factor in Equation 6. While the specific gate voltage dependence is likely impossible to predict in advance, this Figure shows that there is the hope of operationally tuning out some of the large, uncontrolled variations in gate frequencies. In comparing Figure 3 to Figures 1 and 2, we note that the systematic appearance of Figure 3 relies on the fact that the interface in that Figure has a correlation length approximately equal to the total range of 20 nm, so that the random structure in  $\Delta\phi$  apparent in Figures 1 and 2 only appears over the total range of separation in Figure 3.

How can we test the complex valley phase experimentally? First of all, it appears that the global phase (i.e.,  $\phi_L$ ) is not measurable, because there is no physical realizable corresponding to it. We suggest three possible experiments for testing  $\Delta\phi$ : i) Measurements in a 1e2d charge qubit<sup>[28]</sup> could be done as a function of multi-

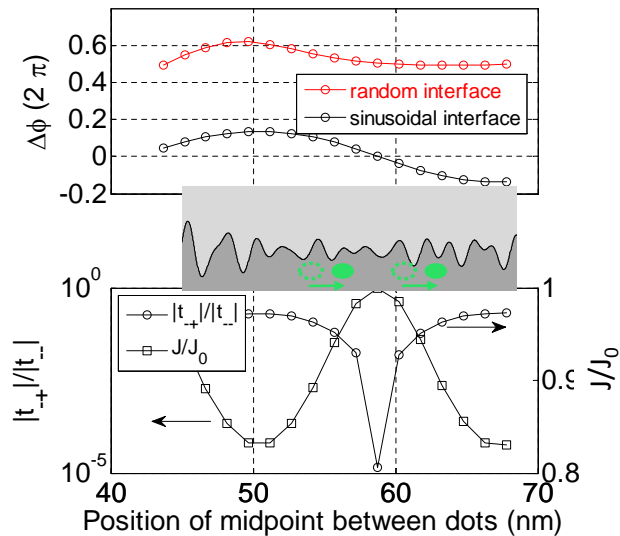


FIG. 3: Large, uncontrolled deviations in gate frequencies/initialization, and voltage control: Lower panel shows the large range of values for both exchange energy  $J$  and inter-valley tunneling energy  $t_{-+}$ ; since each value of  $J$  and  $t_{-+}$  depends on the exact details of the interface roughness, this large range of values corresponds to a large, uncontrolled deviation in the energies. Both panels then show that this large, uncontrolled deviation could be controlled experimentally by using lateral gate voltages to move one or both quantum dots. In this simulation, the separation between the dots is held fixed, to maintain the bare tunneling energy  $t_0$  as a constant.

ple lateral gate voltages, in such a way as to keep the separation between the two dots constant, so that the tunneling matrix element between the two dots would be constant. If  $|t_{-+}| \propto \sqrt{1 + \cos \Delta\phi}$  as predicted in

Equation 7, then the frequency of the charge qubit Rabi oscillations would have the same strong dependence on lateral gate voltage.; ii) Measurements of the exchange energy splitting  $J$  (references [29][30]) in a DQD could be done as a function of multiple lateral gate voltages in the same way as described above. If  $J$  changes in a systematic way with the lateral position of both dots, this would indicate the likelihood of valley phase-mediated modulation of  $J$ ; iii) Very recently, valley blockade in a double quantum dot (DQD), exactly analogous to Pauli spin blockade[31][32][29]), has been reported[33]. In this work, an asymmetry in the size of the bias triangles in a DQD is attributed to blockade in one bias direction due to the impossibility of inter-valley tunneling. Such valley blockade depends on  $\Delta\phi = 0$ , and thus the leakage current in the blocked region  $I_{\text{leak}} \propto (1 - \cos \Delta\phi)/2$ . Thus, we suggest examining the leakage current magnitude as a function of lateral gate voltage.

Also, we estimate as insignificant the magnitude of spin dephasing (through the dependence of  $J$  on  $\Delta\phi$ ) due to charge noise which would modulate the lateral position of one or both dots: From Figure 3,  $dJ/dx \approx 0.1J_0/(10 \text{ nm})$ , lateral motion  $dx/dV_G \approx (1 \text{ nm}/10 \text{ mV})$ , and a voltage noise magnitude  $\Delta V_G = 1 \mu\text{V}$ , we obtain the noise magnitude  $\Delta J \approx 10^{-6}J_0$ . Finally, one way of suppressing the complex valley phase effects and of increasing the valley splitting magnitude, would be to make devices with perfectly flat atomically sharp terraces as large as  $10\mu\text{m}$ [34][35]. However, it is likely that subsequent growth of  $\text{SiO}_2$  or  $\text{SiGe}$  will lead to substantial roughening of such terraces, and thus it appears likely that these valley phase effects will still be present in typical quantum coherent devices.

It is a pleasure to acknowledge useful discussions with Josh Pomeroy, Mark Stiles, Michael Stewart Jr (all of NIST), Andras Palyi (BUTE), John Gamble (Sandia) and Chris Richardson (LPS).

- 
- [1] F. A. Zwanenburg et al., *Rev. Mod. Phys.* **85**, 961 (2013).
- [2] J. J. L. Morton, D. R. McCamey, M. A. Eriksson, and S. A. Lyon, *Nature* **479**, 345 (2011).
- [3] P. Scarlino et al., *Phys. Rev. Lett.* **115**, 106802 (2015).
- [4] E. Kawakami et al., *Nature Nanotech.* **9**, 666 (2014).
- [5] M. Veldhorst et al., *Nature Nanotech.* **9**, 981 (2014).
- [6] M. Veldhorst et al., *Nature* **526**, 410 (2015).
- [7] C. H. Yang et al., *Nature Comm.* **4**, 2069 (2013).
- [8] X. Hao et al., *Nature Comm.* **5**, 3860 (2014).
- [9] S. Goswami, K. A. Slinker, M. Friesen, L. M. McGuire, J. L. Truitt, C. Tahan, L. J. Klein, J. O. Chu, P. M. Mooney, V. W. van der Weide, et al., *Nature Physics* **3**, 41 (2007).
- [10] T. B. Boykin, G. Klimeck, M. A. Eriksson, M. Friesen, S. N. Coppersmith, P. von Allmen, F. Oyafuso, and S. Lee, *Applied Physics Letters* **84**, 115 (2004), URL <http://scitation.aip.org/content/aip/journal/apl/84/1/10.1063/1.1637718;jsessionid=eQPbre3FvIyOPAdeljAVTNIWa.x-aip-live-03>.
- [11] T. B. Boykin, G. Klimeck, M. Friesen, S. N. Coppersmith, P. von Allmen, F. Oyafuso, and S. Lee, *Phys. Rev. B* **70**, 165325 (2004), URL <http://link.aps.org/doi/10.1103/PhysRevB.70.165325>.
- [12] T. B. Boykin, N. Kharche, and G. Klimeck, *Phys. Rev. B* **77**, 245320 (2008), URL <http://link.aps.org/doi/10.1103/PhysRevB.77.245320>.
- [13] M. Friesen and S. N. Coppersmith, *Phys. Rev. B* **81**, 115324 (2010), URL <http://link.aps.org/doi/10.1103/PhysRevB.81.115324>.
- [14] A. L. Saraiva, M. J. Calderón, X. Hu, S. Das Sarma, and B. Koiller, *Phys. Rev. B* **80**, 081305 (2009), URL <http://link.aps.org/doi/10.1103/PhysRevB.80.081305>.
- [15] A. L. Saraiva, M. J. Calderón, R. B. Capaz, X. Hu, S. Das Sarma, and B. Koiller, *Phys. Rev. B* **84**, 155320 (2011), URL <http://link.aps.org/doi/10.1103/PhysRevB.84.155320>.

- 1103/PhysRevB.84.155320.
- [16] S. Srinivasan, G. Klimeck, and L. P. Rokhinson, Applied Physics Letters **93**, 112102 (2008), URL <http://scitation.aip.org/content/aip/journal/apl/93/11/10.1063/1.2981577;jsessionid=eQPbre3FvIyOPAdejAVTNIWa.x-aip-live-03>.
  - [17] J. K. Gamble, M. A. Eriksson, S. N. Coppersmith, and M. Friesen, Phys. Rev. B **88**, 035310 (2013), URL <http://link.aps.org/doi/10.1103/PhysRevB.88.035310>.
  - [18] D. Culcer et al., Phys. Rev. B **82**, 205315 (2010).
  - [19] M. Friesen, S. Chutia, C. Tahan, and S. N. Coppersmith, Phys. Rev. B **75**, 115318 (2007), URL <http://link.aps.org/doi/10.1103/PhysRevB.75.115318>.
  - [20] M. Friesen, M. A. Eriksson, and S. N. Coppersmith, Applied Physics Letters **89**, 202106 (2006), URL <http://scitation.aip.org/content/aip/journal/apl/89/20/10.1063/1.2387975;jsessionid=e8uHB9fAjy0HD4RgKZM7PzA+.x-aip-live-03>.
  - [21] Y. Wu and D. Culcer, Phys. Rev. B **86**, 035321 (2012), URL <http://link.aps.org/doi/10.1103/PhysRevB.86.035321>.
  - [22] D. Culcer et al., Phys. Rev. B **82**, 155312 (2010).
  - [23] W. Huang, M. Veldhorst, N. M. Zimmerman, A. S. Dzurak, and D. Culcer (2016), unpublished.
  - [24] P. Boross, G. Szchenyi, D. Culcer, and A. Plyi, Phys. Rev. B **94**, 035438 (2016).
  - [25] N. Ikarashi and K. Watanabe, Jpn. J. Appl. Phys. **39**, 1278 (2000).
  - [26] O. L. Krivanek and J. H. Mazur, Appl. Phys. Lett. **37**, 392 (1980).
  - [27] W. R. Anderson et al., Micro. Eng. **22**, 43 (1993).
  - [28] T. Hayashi et al., Phys. Rev. Lett. **91**, 226804 (2003).
  - [29] B. Weber et al., Nature Nano. **9**, 430 (2014).
  - [30] J. R. Petta et al., Science **309**, 2180 (2005).
  - [31] N. S. Lai et al., Sci. Rep. **1**, 110 (2011).
  - [32] N. Shaji et al., Nature Physics **4**, 540 (2008).
  - [33] J. K. Perron et al. (2016), unpublished.
  - [34] K. Li et al., J. Vac. Sci. Technol. B **29**, 041806 (2011).
  - [35] S. Tanaka et al., Appl. Phys. Lett. **69**, 1235 (1996).
  - [36] B. G. Streetman, *Solid State Electronic Devices* (Prentice Hall, Englewood Cliffs, NJ, USA, 1995).

## Supplementary Information on Whether the Electron Wavefunction Follows the Interface

In this Section, we will discuss this question as follows:

1. We will give a formal analysis, based on symmetry arguments, that yields the result that the wavefunction follows the interface for any interface slope less than one. This analysis is relevant for the smooth (Si/SiO<sub>2</sub>) interfaces considered in this paper.
2. We will give an estimate based on energy considerations, that yields the result that the wavefunction follows the interface for any interface roughness with correlation length greater than about 0.3 nm. This analysis is relevant for both step (Si/SiGe) and smooth (Si/SiO<sub>2</sub>) interfaces considered in this paper.
3. Based on the two analyses, we will present a result from our simulations where we compare the valley phase for i) an interface with vertical steps to ii) an interface with sloped steps, and show that the valley phase is approximately the same for both interfaces. This result shows that the formal analysis (item 1. above) is thus also relevant for the step (Si/SiGe interfaces).

### A. Symmetry Arguments

The Schrodinger equation in the absence of interface roughness is

$$\left[ -\frac{\hbar^2 \nabla^2}{2m} + V(\mathbf{r}) \right] \psi_e(\mathbf{r}) = \varepsilon \psi_e(\mathbf{r}), \quad (9)$$

Thus, the second derivatives in the original coordinate system are approximately the same as those in the new system, if  $\left| \frac{\partial z'}{\partial x, y} \right| \ll 1$ . In this case, we can immediately see that  $\psi_e(x, y, z) \approx \psi_{e,0}(x, y, z - \zeta(x, y))$ . In summary, if the slope of any interface roughness is substantially less than one, the electron wavefunction will approximately follow the interface.

where  $\psi_e$  is the total electron wavefunction (represented as  $D_\xi(x, y, z)$ ) in Equation 3 in the main text. The solution to this equation is  $\psi_{e,0}(\mathbf{r})$ , the solution for a flat interface.

We wish to examine the effect on  $\psi_e$  when the interface becomes rough, and in particular on the amount by which the spatial derivatives change. We can define new coordinates

$$\begin{aligned} x' &= x \\ y' &= y \\ z' &= z - \zeta(x, y). \end{aligned} \quad (10)$$

The differentials transform as

$$\begin{aligned} \frac{\partial \psi_e}{\partial x} &= \frac{\partial \psi_e}{\partial x'} \frac{\partial x'}{\partial x} + \frac{\partial \psi_e}{\partial z'} \frac{\partial z'}{\partial x} = \frac{\partial \psi_e}{\partial x'} + \frac{\partial \psi_e}{\partial z'} \frac{\partial z'}{\partial x} \\ \frac{\partial \psi_e}{\partial y} &= \frac{\partial \psi_e}{\partial y'} \frac{\partial y'}{\partial y} + \frac{\partial \psi_e}{\partial z'} \frac{\partial z'}{\partial y} = \frac{\partial \psi_e}{\partial y'} + \frac{\partial \psi_e}{\partial z'} \frac{\partial z'}{\partial y} \\ \frac{\partial \psi_e}{\partial z} &= \frac{\partial \psi_e}{\partial z'} \frac{\partial z'}{\partial z} = \frac{\partial \psi_e}{\partial z'}. \end{aligned} \quad (11)$$

The second differentials become

$$\begin{aligned} \frac{\partial}{\partial x} \frac{\partial \psi_e}{\partial x} &= \left( \frac{\partial}{\partial x'} + \frac{\partial z'}{\partial x} \frac{\partial}{\partial z'} \right) \left( \frac{\partial \psi_e}{\partial x'} + \frac{\partial \psi_e}{\partial z'} \frac{\partial z'}{\partial x} \right) = \left[ \frac{\partial^2 \psi_e}{\partial x'^2} + 2 \frac{\partial^2 \psi_e}{\partial x' \partial z'} \frac{\partial z'}{\partial x} + \frac{\partial^2 \psi_e}{\partial z'^2} \left( \frac{\partial z'}{\partial x} \right)^2 \right] \\ \frac{\partial}{\partial y} \frac{\partial \psi_e}{\partial y} &= \left( \frac{\partial}{\partial y'} + \frac{\partial z'}{\partial y} \frac{\partial}{\partial z'} \right) \left( \frac{\partial \psi_e}{\partial y'} + \frac{\partial \psi_e}{\partial z'} \frac{\partial z'}{\partial y} \right) = \left[ \frac{\partial^2 \psi_e}{\partial y'^2} + 2 \frac{\partial^2 \psi_e}{\partial y' \partial z'} \frac{\partial z'}{\partial y} + \frac{\partial^2 \psi_e}{\partial z'^2} \left( \frac{\partial z'}{\partial y} \right)^2 \right] \\ \frac{\partial}{\partial z} \frac{\partial \psi_e}{\partial z} &= \frac{\partial^2 \psi_e}{\partial z'^2}. \end{aligned} \quad (12)$$

### B. Energy Considerations

Here, we consider the interplay between kinetic and potential energies. For a rough interface, since the accumulation gate produces a potential well in the z-direction at the interface and follows conformally the interface roughness, the electron potential energy will be lowered if the wavefunction follows the interface roughness exactly. On the other hand, the more the wavefunction follows the interface roughness, the larger is the kinetic energy in-

crease. For simplicity, we consider only one lateral direction  $x$ .

Thus, we determine the approximate maximum bending of the electron wavefunction by the constraint

$$\frac{\hbar^2}{2m} \frac{d^2\psi}{dx^2} < \langle \psi | (\mathcal{V} + eFz) | \psi \rangle. \quad (13)$$

Note that, for this inequality, the normalization of the wavefunction is present on both sides, so we will suppress the normalization factor.

We define the following parameters:

$\psi_e$  Total electron wavefunction (as distinguished from effective mass envelope function  $\psi$ ).

$\zeta_e(\mathbf{x})$  Height of center of electron wavefunction (as distinguished from the height of the interface  $\zeta(x)$ ). [See Figure 4]

$\zeta_{e0}$  Amplitude of local bending of electron wavefunction (assumed to be quadratic).

$l_{ce}$  Correlation length of electron wavefunction (as distinguished from the correlation length of the interface).

$U_0$  Band offset between Si and SiO<sub>2</sub>, as in Equation 5 of the main text.

$t$  Vertical thickness of electron 2DEG (inversion layer thickness).

$m$  Effective mass of transverse electron in Si;  $m = 0.2m_e$ .

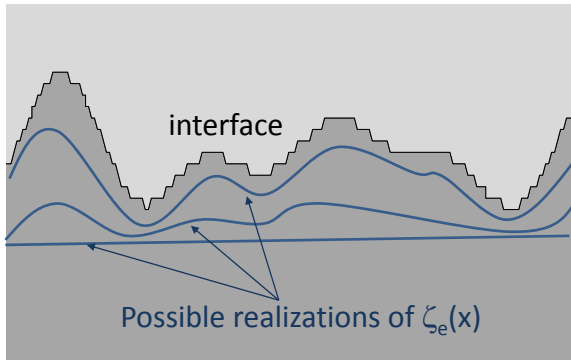


FIG. 4: Figure S1: Possible realizations of  $\zeta_e(x)$ ; the correct realization depends on the interplay between kinetic and potential energy. Bottom curve: kinetic energy term dominates; top curve: potential energy term dominates.

## 1. Kinetic Energy

To approximate the left-hand side of Equation 13, we start by assuming that the wavefunction is locally quadratic:

$$\zeta_e(x) = (\zeta_{e0}) \left( \frac{x}{l_{ce}} \right)^2. \quad (14)$$

Following Equation 3 in the main text, the wavefunction is

$$\psi_e(x, z) = \phi_D(x) \psi(\zeta_e(x) - z) u_\xi(\mathbf{r}) e^{ik_\xi z}. \quad (15)$$

A good approximation to the  $z$ -dependence of the 2DEG is  $\psi(x, z) = e^{-(\zeta_e(x)-z)/t}$  (ref [36]). The contribution to the kinetic energy from the roughness of the 2DEG comes only from this part of the total wavefunction  $\psi_e(x, z)$ :

$$\frac{d^2\psi}{dx^2} = e^{-(\zeta_e(x)-z)/t} \left[ \left( \frac{\zeta_e'}{t} \right)^2 - \frac{\zeta_e''}{t} \right]. \quad (16)$$

With  $\zeta_{e0} \approx 0.5$  nm and  $t \approx 1$  nm, the exponential factor is approximately one, so that

$$\frac{d^2\psi}{dx^2} \approx \left( \frac{\zeta_e'}{t} \right)^2 - \frac{\zeta_e''}{t}. \quad (17)$$

With the quadratic dependence of  $\zeta_e(x)$ , and evaluating at  $x = l_{ce}$ , we obtain

$$\frac{d^2\psi}{dx^2} \approx \left( 2 \frac{\zeta_{e0}}{l_{ce}t} \right)^2 \left[ 1 - \frac{t}{2\zeta_{e0}} \right]. \quad (18)$$

With  $t/\zeta_{e0} \approx 5$  nm / 0.5 nm,

$$\frac{d^2\psi}{dx^2} \approx -2 \frac{\zeta_{e0}}{l_{ce}^2 t}. \quad (19)$$

Finally, the left hand side of Equation 13 is

$$\frac{\hbar^2}{2m} \frac{d^2\psi}{dx^2} \approx -\frac{\hbar^2}{m} \frac{\zeta_{e0}}{l_{ce}^2 t} \quad (20)$$

## 2. Potential Energy

We approximate the vertical potential well at the interface as triangular, with the sloped section having a slope of  $U_0/t$ . The decrease in potential energy when the electron wavefunction is bent with a vertical change of approximately  $\zeta_{e0}$  instead of flat is thus

$$\langle \psi | (\mathcal{V} + eFz) | \psi \rangle \approx \frac{U_0 \zeta_{e0}}{t}. \quad (21)$$

### 3. Summary

Combining Equations 13, 20, 21, we thus obtain a constraint on the minimum radius of curvature or correlation length of the electron wavefunction

$$l_{ce}^2 > \frac{\hbar^2}{mU_0}; \quad (22)$$

using the values in this section ( $U_0 = 3$  eV for Si/SiO<sub>2</sub>), we finally obtain  $l_{ce} > \approx 0.3$  nm. Given that the typical amplitude of roughness is less than or of order 1 nm, this condition is quite similar to that in the previous argument based on symmetry considerations.

### C. Results from Simulations

Figure 5 shows two choices for  $\zeta_e(x)$ , with the smoothed one obeying the approximate constraints derived in the last two sections. We simulated the phase difference, and got the result

$$\Delta\phi_{sharp} = -0.110(2\pi), \Delta\phi_{smoothed} = -0.111(2\pi). \quad (23)$$

Thus, the results of a combination of i) two theoretical constraints on the sharpness of the electron wavefunction as viewed through  $\zeta_e(x)$ , and ii) the very small phase difference for the sharp versus smoothed electron wavefunctions, demonstrate that our assumption in the main text (that the electron wavefunction follows the interface roughness) does not present a significant offset in our results.

### D. Files

All pathnames are relative to L:/internal/SET\_team/Neil/other peoples documents/Culcer/valleys 14.5

**Text:** /manuscript/text/Culcer\_valley\_phase\_v.2.tex.

**All figures** /manuscript/figures/15.11 portrait Culcer phase figures.pptx.

**Fig 1 Main:** /manuscript/figures/Delta phi plots/Step\_NonVicinal.dat and Step\_Vicinal.dat using do\_plot\_step\_vicinal.m.

**Fig 2 Main:** /manuscript/figures/Delta phi plots/Sin\_NonVicinal.dat and Sin\_Vicinal.dat using do\_plot\_sin\_vicinal.m.

**Fig 3 both panels** manuscript/figures/voltage control/VoltageControl\_XL10.dat and \_XL0.dat using do\_plot\_voltage\_control.m.

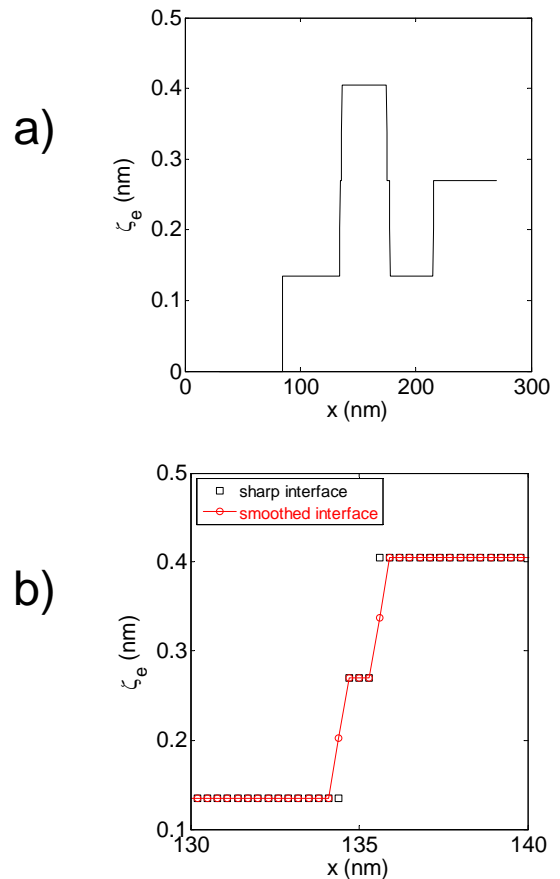


FIG. 5: Figure S2: Sharp and smoothed vertical centers  $\zeta_e(x)$  of electron wavefunction, for testing dependence of  $\Delta\phi$  on the extent to which electron wavefunction follows interface roughness. a) Full extent of sharp  $\zeta_e(x)$  for Si/SiGe simulated interface; quantum dots are centered at 125 and 175 nm, with dot radius  $a = 10.4$  nm; b) Small region of interface, showing smoothing of the original sharp  $\zeta_e(x)$  to give a slope less than one, or a correlation length greater than 0.3 nm.

**Fig S1** /manuscript/figures/15.11 portrait Culcer phase figures.pptx.

**Fig S2** /manuscript/figures/smoothed for Supp/xi\_x\_steps\_tilt\_0\_rand\_1.dat, using do\_plot\_smoothed\_unsmoothed.m, followed by xli, cla, plot(x, y, 'k-')